Hindawi Publishing Corporation
International Journal of Corrosion
Volume 2013, Article ID 824659, 11 pages
http://dx.doi.org/10.1155/2013/824659

Research Article

Combating Corrosion Degradation of Turbine Materials Using HVOF Sprayed 25% (Cr_3C_2-25(Ni20Cr)) + NiCrAlY Coating

N. Jegadeeswaran,[1] M. R. Ramesh,[2] and K. Udaya Bhat[1]

[1] *Metallurgical & Materials Engineering Department, National Institute of Technology Karnataka, Surathkal 575025, India*
[2] *Mechanical Engineering Department, National Institute of Technology Karnataka, Surathkal 575025, India*

Correspondence should be addressed to K. Udaya Bhat; udayabhatk@gmail.com

Received 16 July 2013; Revised 27 September 2013; Accepted 29 September 2013

Academic Editor: Ramazan Solmaz

High velocity oxy fuel process (HVOF) is an advanced coating process for thermal spraying of coatings on to components used in turbines. HVOF process is a thermal spray coating method and is widely used to apply wear, erosion, and corrosion protective coatings to the components used in industrial turbines. 25% (Cr_3C_2-25(Ni20Cr)) + NiCrAlY based coatings have been sprayed on to three turbine materials, namely, Ti-31, Superco-605, and MDN-121. Coated and uncoated substrates were subjected to hot corrosion study under cyclic conditions. Each cycle consisted of 1 hour heating at 800°C followed by 20 minutes air cooling. Gravimetric measurements were done after each cycle and a plot of weight gain as a function of number of cycles is drawn. Parabolic rate constants were estimated for the understanding of corrosion behaviour. It was observed that coated Ti-31 and MDN-121 were more resistant compared to the uncoated ones. Uncoated superco-605 was undergoing sputtering during corrosion study and hence comparison between coated and uncoated superco-605 was difficult. The cross-sectional analysis of the corroded, coated samples indicated the presence of a thin layer of chromium oxide scale on the top of the coating and it imparted better corrosion resistance. Parabolic rate constants also indicated that coating is more beneficial to Ti-31 than to MDN-121.

1. Introduction

Superalloys are extensively used in gas turbine engines, particularly in combustion zone which is subjected to high temperature and long periods of working time [1–3]. Hot corrosion has become a major degradation mechanism (solid salt deposit on the component Type I hot corrosion) in turbines which are operated with low grade fossil fuels [4–6]. To protect the components from degradation and to prolong their life, coatings are commonly used on the blades and vanes of gas turbines [7].

Use of mechanical blend carbide alloy powder as a coating material is highly promising [8]. A cermet system like Cr_3C_2-NiCr is a strong contender for coating applications requiring higher wear, abrasion, and wear resistance. Cr_3C_2 imparts wear, abrasion, and wear resistance and NiCr acts as a metal binder providing necessary coating toughness. It also has good thermal conductivity and hence helps in reducing cooling requirements. Alloy, NiCrAlY, is used in coating applications for imparting oxidation resistance and it reduces thermal mismatch between coating and the substrate [9, 10]. The alloy, NiCrAlY, is used as a bond coat in thermal barrier systems (TBCs) to minimize the mismatch in the coefficient of thermal expansion [11, 12]. (Cr_3C_2-NiCr) + NiCrAlY coatings offers a combination of better wear, abrasion, corrosion, and oxidation resistance, a higher operating temperature up to 850°C, and minimum stress at the interface due to thermal expansion mismatch during thermal cycling [13, 14]. Though some research shows satisfactory results by using Cr_3C_2-NiCr mixture as a coating system, much debate still exists over the best hard phase/composition/matrix ratio for obtaining optimum properties essential for a high temperature coating system [14–16]. This investigation is on the use of carbide alloy powder 25 wt% (Cr_3C_2-25(Ni20Cr)) mechanically blended with NiCrAlY alloy powder (75% by weight) as a coating material for high temperature applications.

The coating properties are influenced not only by the properties of the powders used but also significantly by the spray process and parameters [17, 18]. In this investigation,

Table 1: Chemical compositions of the substrates used for HVOF coatings.

Sl. no.	Alloy material	Chemical composition, wt%
1	Ti-31	Ti-bal, Al-6, V-4
2	Superco-605	Co-bal, Fe-3, Ni-10, Cr-20, Mn-1.5, W-15, Si-0.3
3	MDN-121	Fe-bal, Ni-0.8, Cr-12, Mo-1, Mn-0.6, C-0.2

high velocity oxy fuel (HVOF) process is used for coating spraying. Compared to other spray coatings, such as flame spraying and plasma spraying, HVOF spraying produces a coating having a better bond strength with the substrate [17–20].

The present investigation is an attempt to evaluate the molten salt corrosion of HVOF sprayed 25% (Cr_3C_2-25(Ni20Cr)) + NiCrAlY alloy coated Ti-31, Superco-605, and MDN-121 at 800°C under cyclic conditions in the presence of the Na_2SO_4-50%V_2O_5 salt mixture.

2. Experimental

2.1. Substrate Material and Coating Formulation. The alloys Ti-31, Superco-605, and MDN-121 were used as the substrate materials, in the present study. The equivalent ASTM standards of the substrate materials are ASTM B338 Grade 5, ASTM F90-09, and ASTM A565 Gr616, respectively. The materials were purchased from MIDHANI, Hyderabad, India, in rolled form. The nominal chemical compositions of the substrate materials are given in Table 1. The specimens with dimensions of the approximately 25 mm × 25 mm × 5 mm were cut, ground, and subsequently grit blasted with alumina powders (Grit 45) before spraying of the coatings by HVOF process. This was done to enhance adhesion of the coating to the substrate. The specimen was prepared manually without any structural changes. Figure 1 shows micrographs of the three substrates used for the HVOF coatings.

Commercially available cermet powder (chromium based) was used as the feedstock alloy for HVOF spraying. The details of the feedstock alloy used and HVOF coating are given in Table 2. The powder was mechanical blend type and manufactured by M/s Sultzer Metco Ltd. The coatings were sprayed at Anod Plasma Industries, Kanpur, India. A Metco DJ2600 (India) gun was used for powder spraying. The spray parameters used for HVOF spraying were oxygen flow rate: 270 LPM; LPG flow rate: 70 LPM; air flow rate: 700 LPM; spray distance: about 20 cm; powder feed rate: 50 g/min; fuel pressure: 7 kg/cm^2; air pressure: 5.5 kg/cm^2; oxygen pressure: 10 kg/cm^2; nitrogen gas (powder carrying gas) pressure: 5 kg/cm^2. During HVOF spraying, the specimen was cooled with compressed air.

2.2. Molten Salt Hot Corrosion Test. Hot corrosion studies were conducted at 800°C in a laboratory silicon carbide tube furnace with an accuracy of ±5°C. Physical dimensions of the specimen were recorded carefully with a vernier caliper,

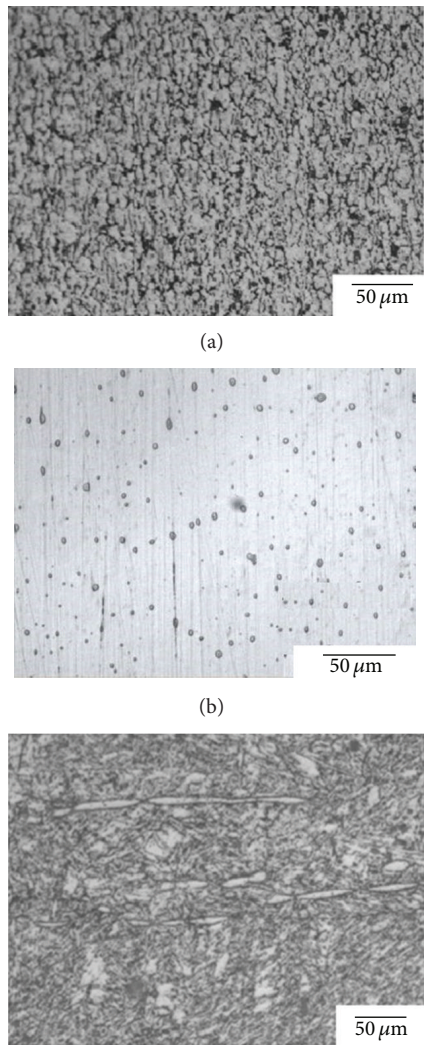

Figure 1: Optical micrograph of substrate materials. (a) Ti-31, (b) Superco-605, and (c) MDN-121.

to evaluate their surface area. Subsequently, specimens were washed with acetone and dried in hot air by means of heating both boat and specimen in an oven at 150°C for about 30 minutes, to remove the moisture. A coating of uniform thickness was applied on to the dry surface, using a camel hairbrush, both on bare substrates and HVOF coated surfaces. The coating mixture was Na_2SO_4-50%V_2O_5 (ratio by weight) and coverage was 3–5 mg/cm^2. During experimentation the prepared specimens were kept in an alumina boat and the weight of the boat and specimen was measured. The hot corrosion studies, under cyclic conditions, were conducted in molten salt environment of above composition. The tests were conducted for 50 cycles of which each cycle consists of 1 hour heating at 800°C in silicon carbide tube furnace followed by 20 min cooling in air.

The weight change values were measured at the end of each cycle with the aim to understand the kinetics of corrosion. Visual observations were made after the end of each

Table 2: Composition of the feedstock alloys, coating thickness, and porosity.

Chemical composition (wt%)	Particle size (μm) Shape	Average coating thickness (μm)	Porosity	Microhardness (Hv)
25% (Cr_3C_2-25(Ni20Cr)) + 75% (Bal Ni-21Cr-8Al-0.5Y)	−45 + 15 Spherical	306	<1.5%	553

(a) (b) (c)

Figure 2: Optical macrograph of 25% (Cr_3C_2-25(Ni20Cr)) + NiCrAlY coated materials. (a) Ti-31, (b) Superco-605, and (c) MDN-121. Dimension of the samples: 25 mm × 25 mm.

cycle with respect to colour, luster, or any other physical aspects of the oxide scales being formed. The reproducibility in the experiment was established by repeating the experiments. The corrosion products of the uncoated (bare) and HVOF coated materials are analyzed by using X-ray diffractometer (XRD), scanning electron microscope (SEM), and energy dispersive X-ray spectroscope (EDX) to reveal their microstructural and compositional features and for elucidating the corrosion mechanisms.

3. Results and Discussion

3.1. Analysis of As-Coated Specimen. Figure 2 shows optical macrographs of the as-coated specimens, namely, coated Ti-31, coated Superco-605, and coated MDN-121. The coatings appeared as dark grey in colour. The coatings were smooth and roughness measurements using a stylus based profilemeter showed a Ra value in the range of 6–8 μm. The typical morphological features of as-coated surface shown in Figure 3 indicate that the coating is partially molten and resolidified. Similar morphological features are reported in the case of HVOF sprayed coatings by Sidhu et al. [20–22], Lotfi [23], and Yuan et al. [24]. The micrograph in Figure 3 shows the presence of chromium carbide particles distributed in the matrix which is rich with melted Ni. There are no pores and cavities which are highly penetrating towards the substrate. Occasional cracks were observed but they are limited to top surface only. The EDX analysis of the coating indicates that the coating is rich in Cr and Ni and that some amount of oxidation has taken place during HVOF spraying. By cross-sectioning the coatings followed by metallographic polishing and observation using scanning electron microscope, the coating thickness was measured and the thickness was in the range of

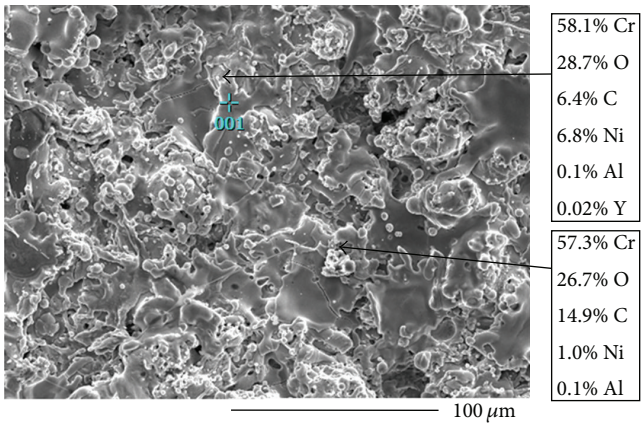

Figure 3: Typical morphology of the cermet coated surface.

300–310 μm. A typical cross-sectional micrograph is shown in Figure 4. The coating is reasonably dense and the features are typical of HVOF coatings. We see partially molten splats impinging the substrate surface and suddenly solidifying. Splat formation mainly depends on the velocity of the impacting particles, their temperature, extent of oxidation, and chemical complexity of the particles [25, 26]. The substrate-coating interface is good. Only small cavities are observed. Good contact between coating and substrate also indicates that the cooling of the splat layer is fast [25]. There are no direct channels passing through the coating and allowing the substrate to be in contact with the atmosphere.

Figure 4 also shows the laminar pattern in which the coating was deposited during HVOF spraying. The coatings were deposited on a stationary substrate by moving HVOF gun

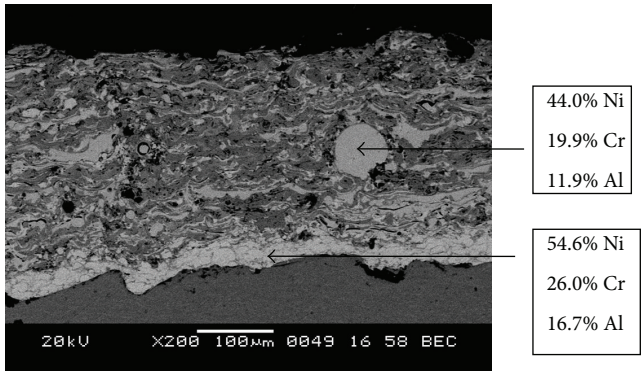

Figure 4: Cross-sectional image showing the nature of HVOF sprayed coatings.

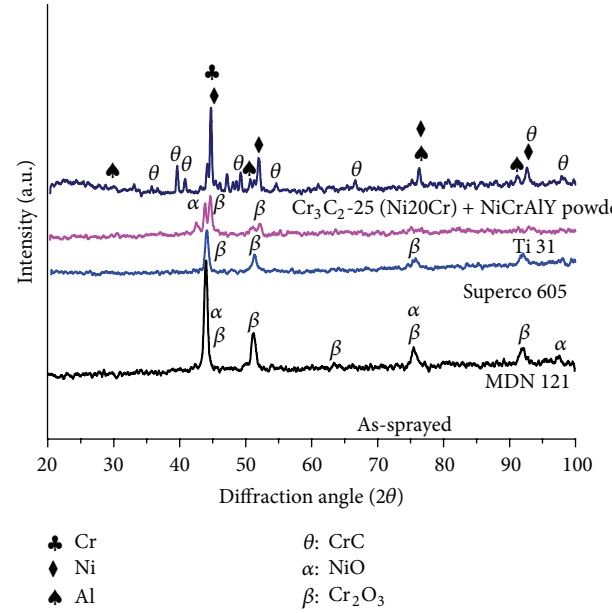

Figure 5: XRD profiles of mechanically blend 25% (Cr_3C_2-25(Ni20Cr)) + NiCrAlY powder and HVOF sprayed coatings on three substrates are shown.

(rastering) and the required thickness was achieved by varying the number of passes. In the cross-sectional micrograph shown in Figure 4 dark areas corresponds to porosity and voids. Voids are visible, both in the coating and at the coating-substrate interface. Similar microstructural features in HVOF sprayed coatings are reported by Sidhu et al. [21, 27]. The EDX analysis at various locations across the thickness shows that coating is rich in elements like Ni, Cr, and Al. Clear peaks corresponding to chromium carbides are visible in the plot.

Figure 5 shows results of XRD analysis on coatings sprayed over different substrates. The 2θ reflections clearly indicate that the coating is rich in terms of oxides of Ni and Cr. Comparing with the XRD profiles of initially used powder we conclude that during spraying the particles have undergone oxidation along with partial melting. These oxides are predominantly oxides of Ni and Cr. Neiser et al. [28] have reported that the oxidation of the elements during thermal spraying is controlled by transport phenomena.

3.2. Hot Corrosion Studies on Coated and Uncoated Substrates

3.2.1. Visual Observations and Thermogravimetric Analysis. The macrographs of samples of uncoated Ti-31, Superco-605, and MDN-121 and the HVOF sprayed 25% (Cr_3C_2-25(Ni20Cr)) + NiCrAlY coatings on the Ti-31, Superco-605, and MDN-121 alloys which are subjected to hot corrosion in Na_2SO_4-50%V_2O_5 environment for 50 cycles at 800°C are illustrated in Figure 6. It is noted that there was formation of oxide scales on the surface of Ti-31 from the first cycle itself; on the 23rd cycle, the surface appeared brownish. Severe spalling of oxide scales was observed from 31st cycle onwards. The surface of Superco-605 started to become grey in colour whereas the surface of the MDN-121 started to change into shiny grey in colour. The colour of the as-sprayed coating was grey which turned into brownish colour during the first cycle of exposure to salt environment.

The plots of cumulative weight gain (mg/cm^2) as a function of time expressed in number of cycles for uncoated substrates are shown in Figure 7(a) and for cermet coated substrates in Figure 7(b). In the case of uncoated Ti-31 and MDN-121, the weight gains at the end of 50 cycles are found to be 75.8 and 2.7 mg/cm^2, respectively. Uncoated Superco-605 exhibited weight loss during the complete cycles of hot corrosion studies as a result of intense spalling and sputtering of the oxide scale. Spalling and sputtering also made it difficult to measure the overall weight gain. Tiwari and Prakash [29] and Singh et al. [30] have reported that scale on the superco-605 exposed to Na_2SO_4-60%V_2O_5 is highly prone to cracking. Also, Anuwar et al. [2] have reported a weight gain of about 72 mg/cm^2 after 60 cycles of hot corrosion at 750°C in presence of Na_2SO_4-60%V_2O_5 for uncoated Ti-31.

The values of overall weight gain after 50 cycles of hot corrosion for 25% (Cr_3C_2-25(Ni20Cr)) + NiCrAlY coated Ti-31, Superco-605, and MDN-121 are found to be 1.5, 1.3, and 1.25 mg/cm^2, respectively. Though a small difference exists in weight gain for different coated substrates, the net weight gain for all coated materials is less compared to weight gain for uncoated substrates. In other words, cermet coating can protect the substrates from the attack of molten Na_2SO_4-50%V_2O_5 salt mixture. Further, to explore the possibility of parabolic relationship between weight gain and time of exposure, square of weight gain (mg^2/cm^4) data is plotted as a function of time [31–34]. They are shown in Figure 8(a) for uncoated substrates and in Figure 8(b) for coated substrates. The plot shows a clear deviation from the parabolic rate law for the Ti-31. With increase in the number of cycles, the "y axis" value increases rapidly. This indicates that the oxide scale is not much protective in molten salt environment. It is evident from the plot shown in Figure 8(a) that the MDN-121 alloys nearly follow parabolic behavior. The parabolic rate constants, K_p, for the Ti-31 and MDN-121 are $107.6 * 10^{-8}$ and $0.152 * 10^{-8}$ g^2 cm^{-4} s^{-1}, respectively. The parabolic rate constant is very small for Superco-605, but it must be stressed

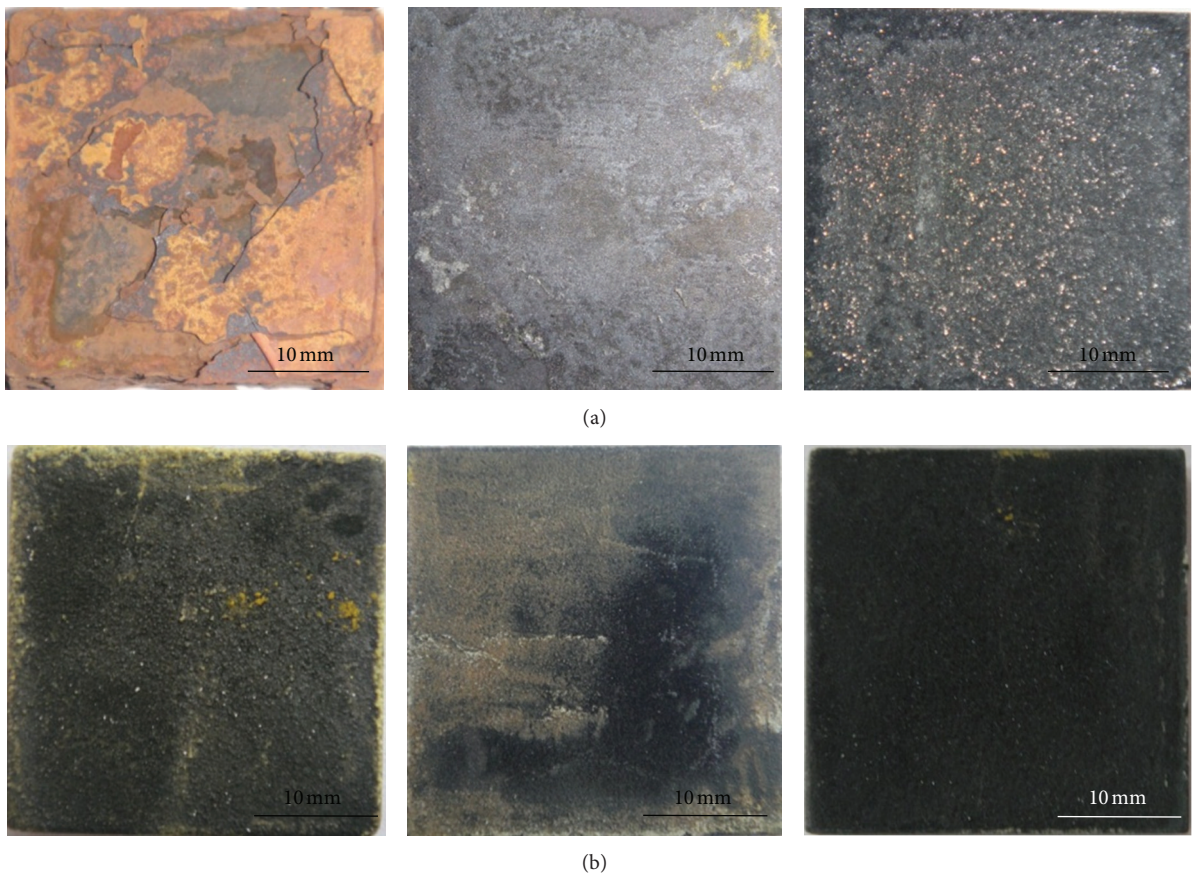

Figure 6: Macrographs of uncoated substrates (top row, in sequence for Ti-31, Superco-605, and MDN-121) and 25% (Cr_3C_2-25(Ni20Cr)) + NiCrAlY coating (bottom row, in sequence for Ti-31, Superco-605, and MDN-121) subjected to hot corrosion in Na_2SO_4-50%V_2O_5 environment at 800°C for 50 cycles.

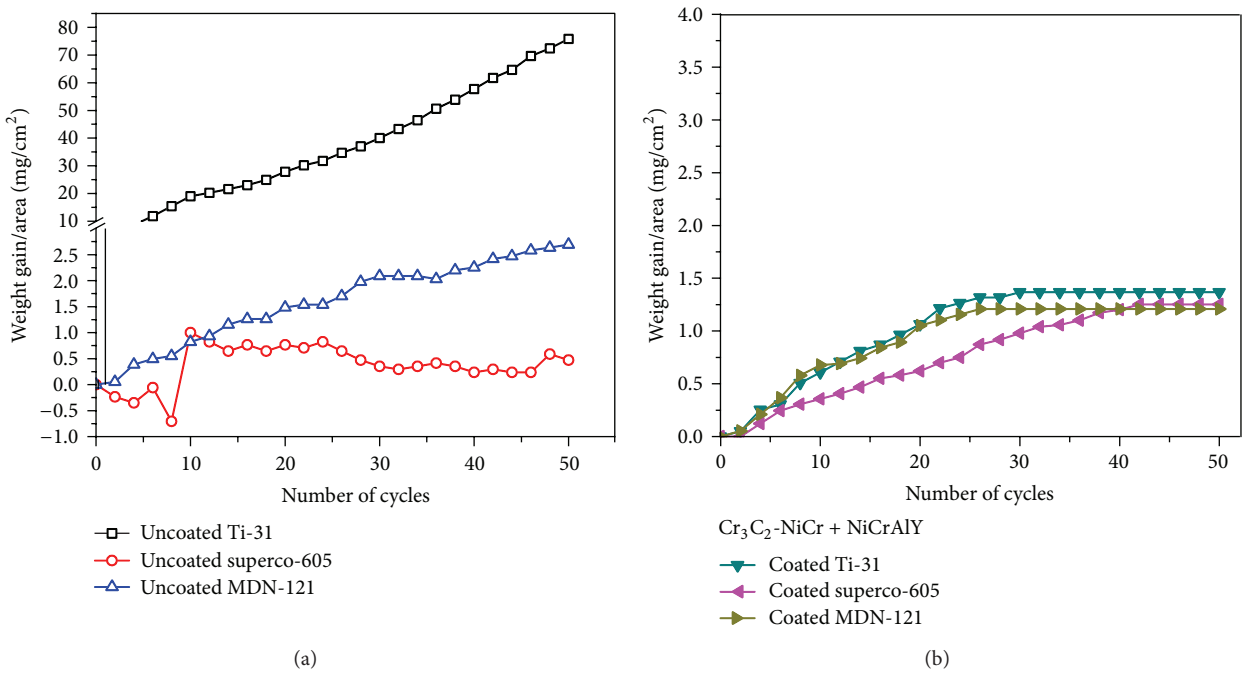

Figure 7: Plots of weight gain per unit area as a function of number of hot corrosion cycles. (a) Uncoated samples, (b) 25% (Cr_3C_2-25(Ni20Cr)) + NiCrAlY coated substrates.

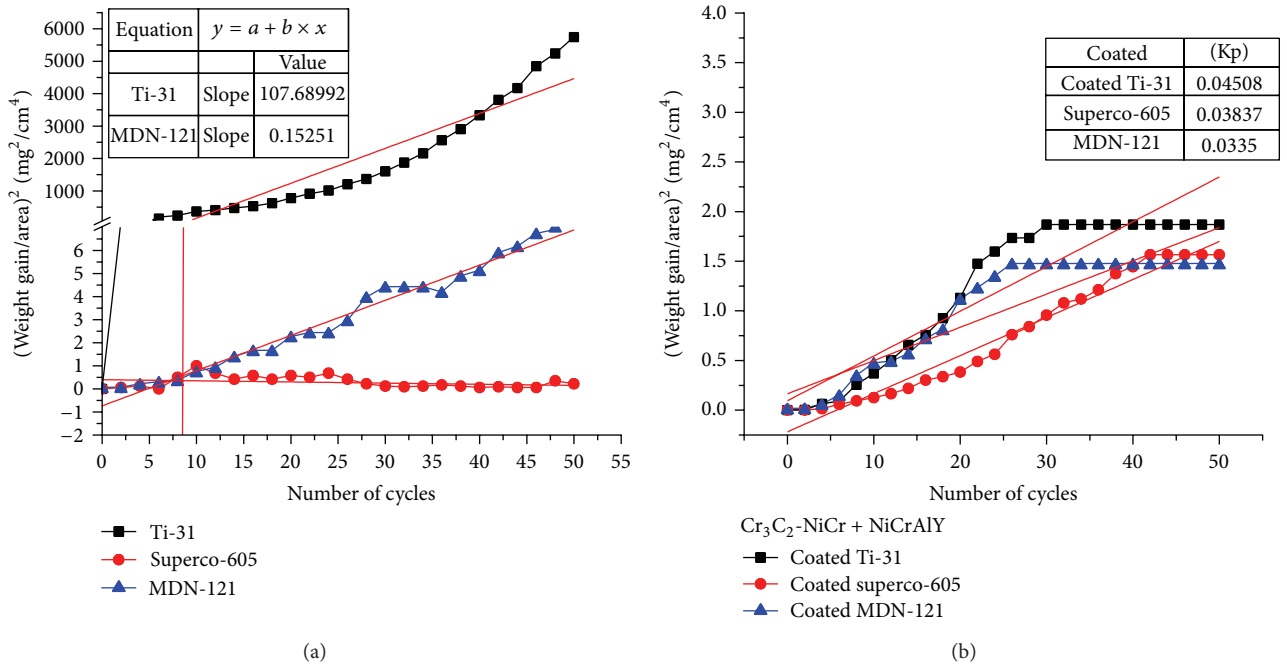

FIGURE 8: Plot of (weight gain/area)^2 versus number of cycles for coated samples subjected to hot corrosion for 50 cycles in Na_2SO_4-50%V_2O_5 environment at 800°C. (a) Uncoated samples, (b) 25% (Cr_3C_2-25(Ni20Cr)) + NiCrAlY coated substrates. Multiplication factor for K_p = 10^{-8} g^2 cm^{-4} s^{-1}).

that weight measurement was very difficult due to the problems of spalling and sputtering. The parabolic rate constants, K_p, for the cermet coated Ti-31, Superco-605, and MDN-121 are $0.045 * 10^{-8}$, $0.0335 * 10^{-8}$, and $0.038 * 10^{-8}$ g^2 cm^{-4} s^{-1}, respectively. The reported values of K_p are upper limit values as they are calculated considering 1 to 50 cycles. Kamal et al. [13] have shown that Cr_3C_2-NiCr coatings on Ni and Fe based superalloys produced by detonation gun spraying improves hot corrosion resistance against Na_2SO_4-60%V_2O_5 at 900°C and the estimated K_p values are of the same order. The low value of K_p also indicates that the coating is protective against Na_2SO_4-50%V_2O_5 environment. The coating becomes saturated after about 30 cycles for coated Ti-31 as well as coated MDN-121 and after 45 cycles for coated superco-605. This again shows that the hot corrosion rate drops as number of cycle increases. This behavior is distinct compared to hot corrosion of bare substrates.

3.2.2. X-Ray Diffraction Analysis. The X-ray diffraction patterns of the top scale, after its exposure to salt environment at 800°C for 50 cycles, are shown in Figure 9. In Figure 9(a), the phases present in the scales of uncoated substrates exposed to salt environment are given. The scales are rich in oxides of Fe, Cr (in corroded MDN-121) oxides of elements like Cr and Co (in corroded superco-605), and oxides of Ti and Al (in corroded Ti-31). Added to that, many other oxides (like Na_2O, $TiVO_4$, WO_3, $FeVO_4$, and FeS_2) are observed as relatively minor phases. Investigation on hot corrosion resistance of Ti-31 in Na_2SO_4-60%V_2O_5 at 750°C by Anuwar et al. [2] also states that oxides of Ti and Al are the major phases in the corrosion product. The scale on the cermet coated Ti-31, Superco-605, and MDN-121 surfaces under study consisted of Cr_2O_3, NiO, and Al_2O_3 as major phases. The coated surfaces also consisted of Na_2O, SO_3, SiO_2, V_2O_5 $AlVO_4$, $NiCr_2O_4$, and NiV_2O_5 as minor phases. Hot corrosion study of plasma sprayed Al_2O_3 dispersed NiCrAlY in Na_2SO_4-50%V_2O_5 at 800°C, by Sreedhar et al. [34] has shown Al_2O_3, NiO, Cr_2O_3, and $NiCr_2O_4$ as major constituents in the corrosion product.

3.3. SEM and EDX Analysis

3.3.1. Surface Analysis. The morphology of the corroded surfaces of uncoated Ti-31, Superco-605, and MDN-121 is shown in Figure 10. All surfaces were relatively smooth. The corroded Ti-31 surface showed a nodular structure and the scale was rich with oxides of Ti and Al. The corroded surface of uncoated Superco-605 showed mud cracks on the surface and the scale was rich with oxides of Na, S, Cr, and Co. The presence of cracks and high levels of S in the scale also indicates that the coating is not adherent and prone to spalling, which is also observed in visual examinations and gravimetric analysis. Amount of Al is not sufficient to form a continuous scale on the surface. Here we have TiO_2 scale with local patches of Al_2O_3. During cyclic heating and cooling, the interface gets opened out and facilitates penetration of oxidizing species. This leads to a high value of weight gain. The corroded surface of uncoated MDN-121 showed extensive broken scales which are rich in oxides of Cr and Fe. It is also noted that presence of 12% Cr in the substrate is not sufficient to form a complete corrosion resistant oxide scale, especially when

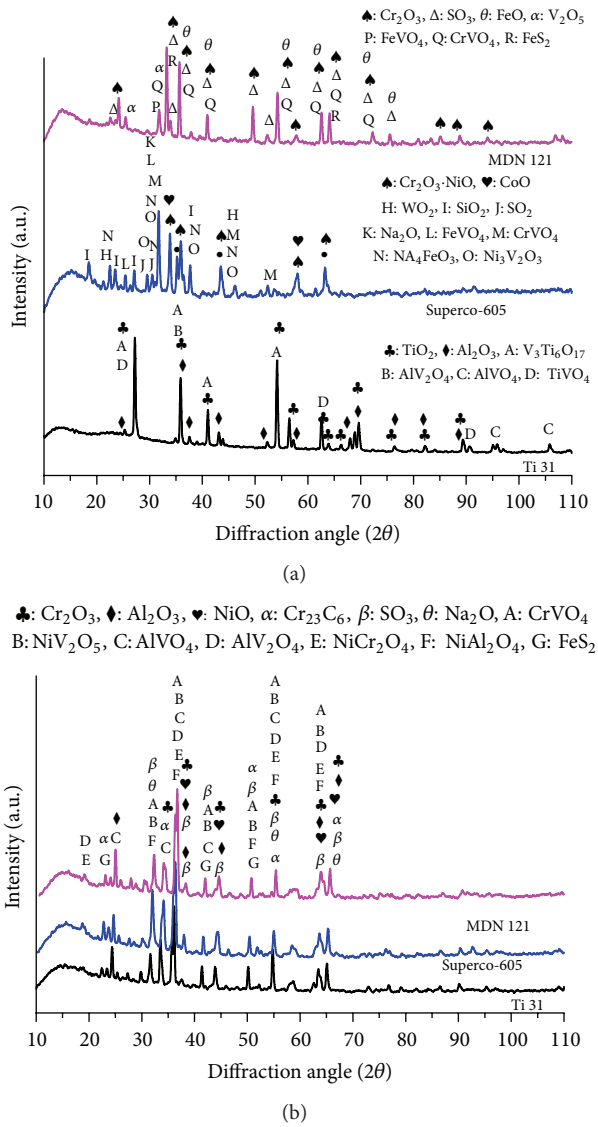

Figure 9: X-ray diffraction patterns. (a) Uncoated alloys, (b) coated 25% (Cr_3C_2-25(Ni20Cr))+NiCrAlY, coated Ti-31, Superco-605, and MDN-121 subjected to hot corrosion in Na_2SO_4-50%V_2O_5 for 50 cycles at 800°C.

carbon percentage is 0.2%. Because of this Fe was also getting oxidized to produce a nonadherent scale and the coating got broke off and opened out during its formation. This lead to formation of fresh oxide scales and this process continued throughout the cyclic corrosion study. The weight gain experiments also showed that the coating growth is rapid and follow a nonparabolic kinetic relationship. The morphologies of the corroded samples coated with cermet coatings are given in Figure 11. In Figures 11(a), 11(b), and 11(c) are the substrates of Ti-31, Superco-605, and MDN-121, respectively. The morphology looks similar in all three cases. Similar morphological features are also reported during hot corrosion of MCrAlYSiB (M=Ni or Co) coated superalloys [35, 36]. Though the coatings look like broken scales (plate like morphology), there was no spalling of the scales. EDX measurement on the scales shows that they are rich in oxides of Cr and Ni. The weight gain measurement presented earlier indicates that the weight gain is smaller compared to that in the case of uncoated substrates. This indicates compactness of the scales on the coated surface. Sreedhar et al. [34] have reported that the plate like morphology is primarily Cr_2O_3 and in between the plates NiO and Al_2O_3. Their coating is NiCrAlY based and the hot corrosion environment is Na_2SO_4-50%V_2O_5. Formation of oxides on the surface of MCrAlY (M=Ni or Co) based coating during hot corrosion in presence of sulphate film is also reported by Jiang et al. [35].

3.3.2. Cross-Sectional Analysis. Figure 12 shows a cross-sectional micrograph of one of the cermet coated specimen exposed to hot corrosion environment. The micrograph shows a clear oxide layer at the top of the coating (marked arrow). The oxide layer is thin compared to total thickness of the coating and it indicates that a major fraction of the coating is unaffected by the hot corrosion environment. Formation of a thin oxide rich layer on the surface of Cr_3C_2-NiCr coating and NiCrAl coating on Ni and Fe based superalloys during hot corrosion is reported by Kamal et al. [13], Jiang et al. [35], and Mahesh et al. [37]. The thickness of the oxide layer is nonuniform and it is attributed to heterogeneity in the microstructure which is due to lack of complete melting and nonhomogeneity of the initial powder. Also, HVOF spraying produces a coating, which is lamellar in nature with distinct splat boundaries oriented parallel to the coating-substrate interface [8, 21, 23]. The EDX analysis (Figure 12(a)) done at various points across the cross-section (Figure 12(b)) also indicates that the top layer (point 1) is rich in oxides. This is marked using an arrow in the "O" mapping shown in Figure 13. In Figure 13 mapping for elements Al, Cr, and Ni are also shown. The mapping clearly indicates nonhomogeneity in the chemical composition. The nonhomogeneity in the composition across the coating is attributed to the reasons explained in previous lines.

3.4. Degradation of HVOF Sprayed Protective Coatings. Cermet, 25% (Cr_3C_2-25(Ni20Cr)) + NiCrAlY based mechanically blend coatings have been applied on to 3 types of substrates used in gas turbines using high velocity oxy fuel (HVOF) process and their hot corrosion resistance was studied. The results clearly indicate that compared to uncoated substrates the coating provides excellent hot corrosion resistance. It is a promising coating developed for the protection of components used in fossil based turbines.

The gravimetric analysis under cyclic hot corrosion study indicates that, the samples continuously gain the weight (Figures 7(a) and 7(b)). The weight gain is more in the initial cycles of corrosion study and the extent of weight gain reduces with successive cycles. The higher weight gain in the first few cycles of corrosion study might be due to the rapid formation of oxides at the grain boundaries and within the pores present at the top layer, due to the penetration of the oxidizing species. Afterwards, the formation of oxides depends on the penetration of oxygen through the existing oxide layers.

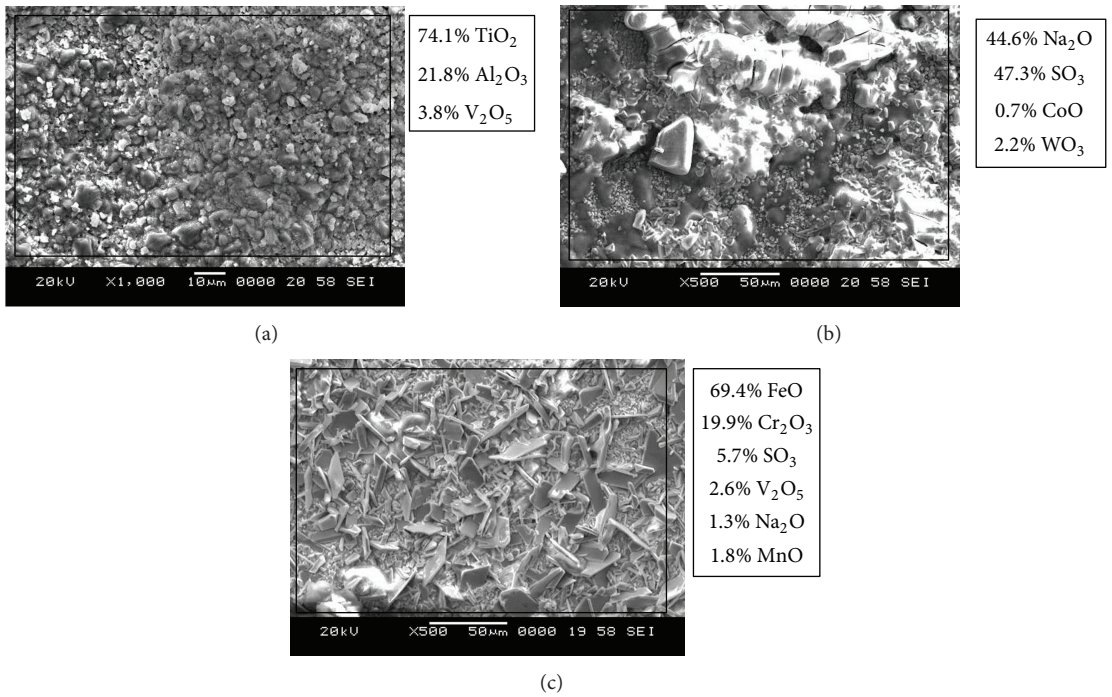

Figure 10: Morphology and EDX analysis of corroded samples. Micrographs corresponding to (a), (b), and (c) are for uncoated Ti-31, Superco-605, and MDN-121 samples, respectively.

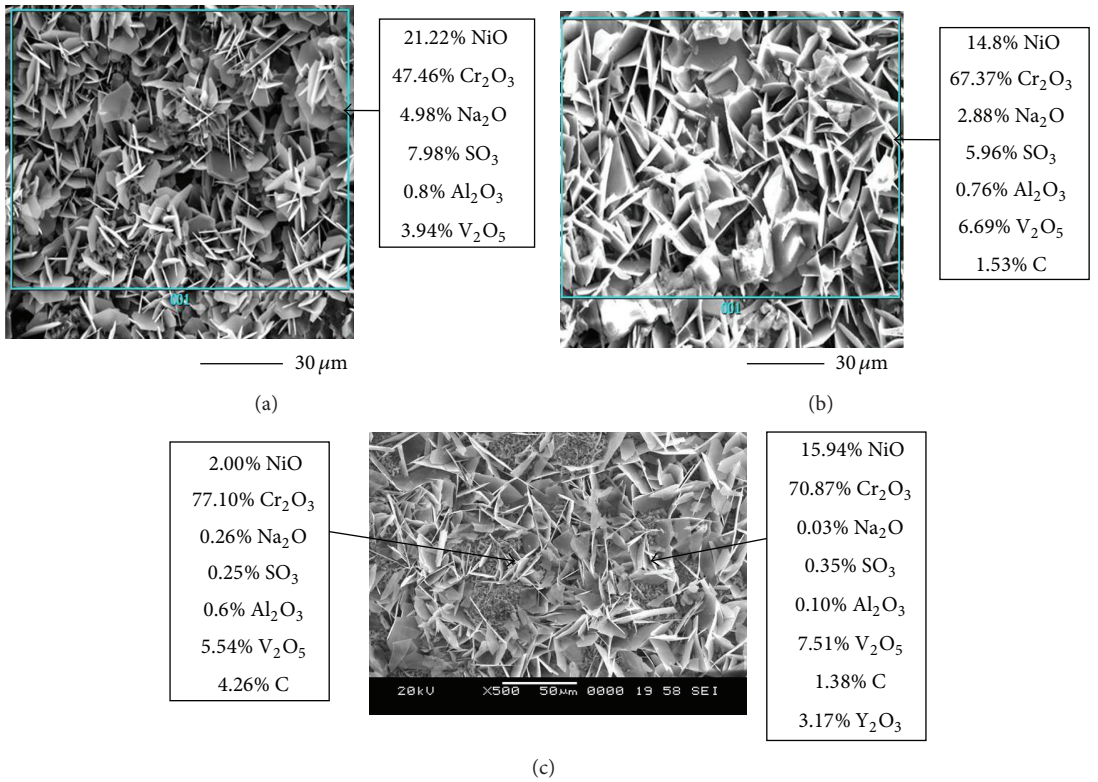

Figure 11: SEM and EDX analysis of 25% (Cr_3C_2-25(Ni20Cr)) + NiCrAlY coated materials subjected to hot corrosion for 50 cycles in Na_2SO_4 + 50%V_2O_5 at 800°C. (a) Ti-31, (b) Superco-605, and (c) MDN-121.

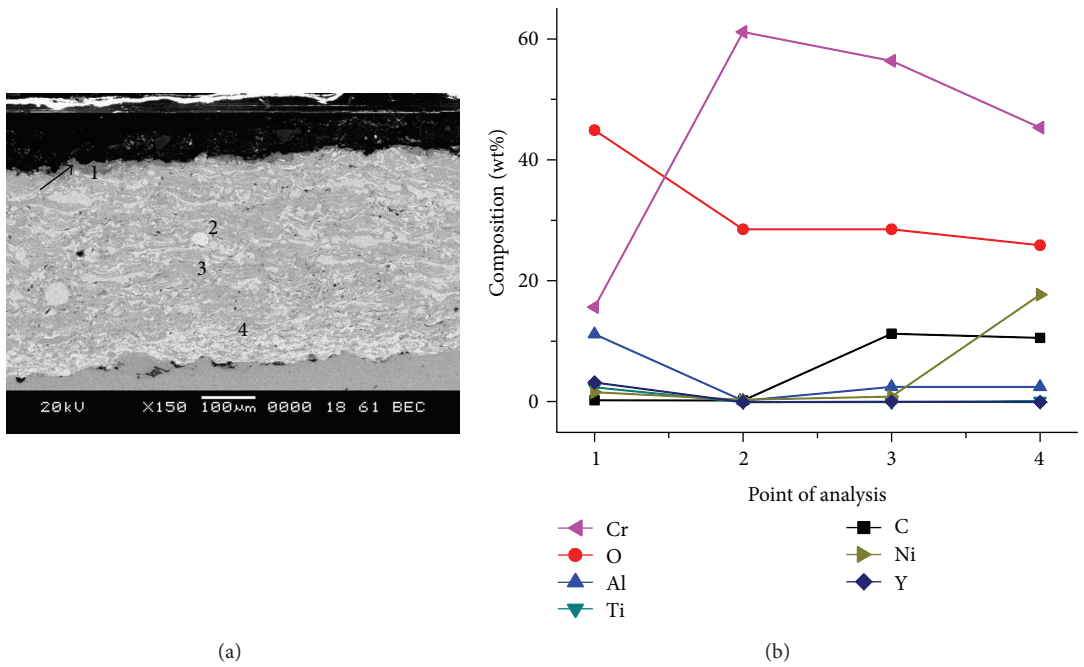

Figure 12: Cross-sectional micrograph of the HVOF coated and hot corroded Ti-31 sample. (a) Micrograph and points of EDX analysis, (b) plots of EDX analysis at various points.

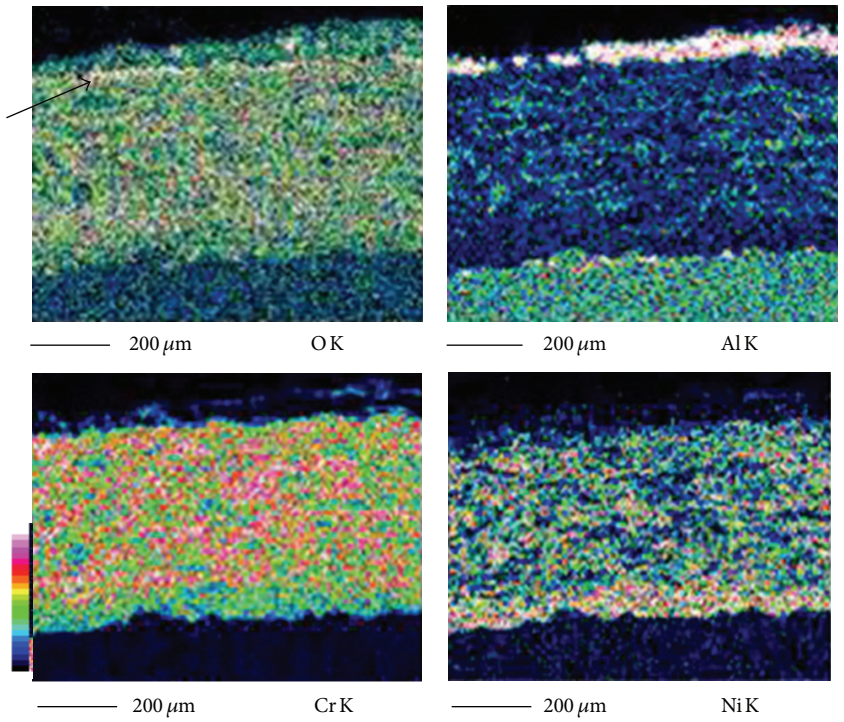

Figure 13: X-ray mapping for the elements of O, Al, Cr, and Ni over the region given in Figure 12(a).

The parabolic rate constants for the hot corroded alloys (Ti-31 and MDN-121) are higher compared to cermet coated alloys (Figures 8(a) and 8(b)). The uncoated Ti-31 alloy undergoes very rapid weight gain compared to HVOF sprayed alloy. It is attributed to nonadherent oxide layer forming at the surface. At the top of Ti-31, a mixture of TiO_2 and Al_2O_3 forms, as the fraction of Al_2O_3 is not sufficient to form a continuous protective oxide layer on the surface. The interface between the oxides is an easy path for oxygen migration and interface gets opened out during cyclic heating and

cooling. End result is a high level of weight gain for uncoated Ti-31. Even in the case of mechanical blend carbide coated samples, the coating reduces weight gain by more than half. Observed low parabolic rate constant for uncoated superco-605 is an artifact introduced due to severe spalling and sputtering. It is reported that formation of Fe_2O_3 during hot corrosion introduces severe strain into the top layer and promotes spalling [13]. In Ni based superalloys, sputtering is reported by Kamal et al. [13]. The superco-605 alloy has about 3 wt% Fe and it will oxidize and introduce strain in the top continuous layer. When strain exceeds the top layer strength, the top layer bursts and gets sputtered out. A large drop in the value of K_p of coated MDN-121 substrate compared to uncoated MDN-121 indicates that the cermet coating is more useful for MDN-121 alloy, compared to Ti-31 alloy.

During hot corrosion, the corroding species, mainly O^{2-}, formed due to the fact that the dissolution of sodium sulphate reacts with the top surface of the coating and starts to migrate through the interface. As the reaction proceeds, the elements like Fe and Ni were oxidized at the top surface but more importantly, Cr gets oxidized into Cr_2O_3. Cr_2O_3 forms a continuous layer and imparts corrosion resistance property [32]. Continuous Cr_2O_3 layer at the top of the coating will not allow further transport of the oxidizing species and metallic ions across it, easily. This reduces availability of oxygen in the underlying layer. Due to this with the passage of time, further corrosion will be reduced. During this process, some of the oxides will undergo reaction within them forming mixed compounds. Compounds like $NiCrO_4$, $CrVO_4$, and $NiAl_2O_4$ are formed because of such reactions.

4. Conclusions

Mechanical blend cermet alloy, 25% (Cr_3C_2-25(Ni20Cr)) + NiCrAlY alloy powder, was successfully coated on alloys used in turbine applications, namely, Ti-31, Superco-605, and MDN-121 alloys, using high velocity oxy fuel process. The coated samples were characterized for microstructural features. The coated and uncoated specimens were subjected to cyclic hot corrosion study at 800°C under the conditions of Na_2SO_4-50 wt%V_2O_5. Weight gain measurements were conducted after each cycle and it showed that coated specimens (Ti-31 and MDN-121) showed minimum weight gain compared to uncoated specimens. Parabolic rate constants were estimated and the value is much lower for coated specimens than for uncoated specimens. It also indicates that for Ti-31, the coating was more beneficial than for MDN-121. The better corrosion protection of coated substrates was attributed to the formation of a top layer consisting of oxides of Cr and Ni. In the case of uncoated Superco-605, there was severe spalling at the surface during cyclic corrosion study and due to this comparison of corrosion resistance between coated and uncoated substrate was difficult.

Conflict of Interests

The authors declare that they have no conflict of interests.

References

[1] H. Cho, D. M. Lee, J. H. Lee, K. H. Bang, and B. W. Lee, "Thermal oxidation behavior of ceramic-coated Ni-Cr-base superalloys," *Surface and Coatings Technology*, vol. 202, no. 22-23, pp. 5625–5628, 2008.

[2] M. Anuwar, R. Jayaganthan, V. K. Tewari, and N. Arivazhagan, "A study on the hot corrosion behavior of Ti-6Al-4V alloy," *Materials Letters*, vol. 61, no. 7, pp. 1483–1488, 2007.

[3] G. R. Krishna, D. K. Das, V. Singh, and S. V. Joshi, "Role of Pt content in the microstructural development and oxidation performance of Pt-aluminide coatings produced using a high-activity aluminizing process," *Materials Science and Engineering A*, vol. 251, no. 1-2, pp. 40–47, 1998.

[4] K. L. Luthra and C. L. Briant, "Mechanism of adhesion of alumina on MCrAlY alloys," *Oxidation of Metals*, vol. 26, no. 5-6, pp. 397–416, 1986.

[5] D. W. McKee and K. L. Luthra, "Plasma-sprayed coatings for titanium alloy oxidation protection," *Surface and Coatings Technology*, vol. 56, no. 2, pp. 109–117, 1993.

[6] I. Gurappa, "Protection of titanium alloy components against high temperature corrosion," *Materials Science and Engineering A*, vol. 356, no. 1-2, pp. 372–380, 2003.

[7] J. H. Lee, P. C. Tsai, and J. W. Lee, "Cyclic oxidation behavior and microstructure evolution of aluminized, Pt-aluminized high velocity oxygen fuel sprayed CoNiCrAlY coatings," *Thin Solid Films*, vol. 517, no. 17, pp. 5253–5258, 2009.

[8] S. S. Chatha, H. S. Sidhu, and B. S. Sidhu, "Characterisation and corrosion-erosion behavior of carbide based thermal spray coatings," *Journal of Minerals and Materials Characterization and Engineering*, vol. 11, no. 6, pp. 569–586, 2012.

[9] N. Eliaz, G. Shemesh, and R. M. Latanision, "Hot corrosion in gas turbine components," *Engineering Failure Analysis*, vol. 9, no. 1, pp. 31–43, 2002.

[10] A. N. Khan and J. Lu, "Behavior of air plasma sprayed thermal barrier coatings, subject to intense thermal cycling," *Surface and Coatings Technology*, vol. 166, no. 1, pp. 37–43, 2003.

[11] H. L. Tsai and P. C. Tsai, "Thermal cyclic response of laser-glazed plasma-sprayed ZrO_2-19.5wt.%Y_2O_3/Ni-22Cr-10Al-1Y thermal barrier coatings," *Materials Science and Engineering A*, vol. 177, no. 1-2, pp. 227–232, 1994.

[12] H. L. Tsai and P. C. Tsai, "Performance of laser-glazed plasma-sprayed (ZrO_2-12wt.%Y_2O_3)/(Ni-22wt.%Cr-10wt.%Al-1wt.%Y) thermal barrier coatings in cyclic oxidation tests," *Surface and Coatings Technology*, vol. 71, no. 1, pp. 53–59, 1995.

[13] S. Kamal, R. Jayaganthan, S. Prakash, and S. Kumar, "Hot corrosion behavior of detonation gun sprayed Cr_3C_2-NiCr coatings on Ni and Fe-based superalloys in Na_2SO_4-60% V_2O_5 environment at 900°C," *Journal of Alloys and Compounds*, vol. 463, no. 1-2, pp. 358–372, 2008.

[14] K. J. Stein, B. S. Schorr, and A. R. Marder, "Erosion of thermal spray MCr-Cr_3C_2 cermet coatings," *Wear*, vol. 224, no. 1, pp. 153–159, 1999.

[15] H. Singh, D. Puri, and S. Prakash, "Some studies on hot corrosion performance of plasma sprayed coatings on a Fe-based superalloy," *Surface and Coatings Technology*, vol. 192, no. 1, pp. 27–38, 2005.

[16] S. Kamal, R. Jayaganthan, and S. Prakash, "Evaluation of cyclic hot corrosion behaviour of detonation gun sprayed Cr_3C_2-25%NiCr coatings on nickel- and iron-based superalloys," *Surface and Coatings Technology*, vol. 203, no. 8, pp. 1004–1013, 2009.

[17] H. S. Sidhu, B. S. Sidhu, and S. Prakash, "Solid particle erosion of HVOF sprayed NiCr and Stellite-6 coatings," *Surface and Coatings Technology*, vol. 202, no. 2, pp. 232–238, 2007.

[18] G. Bolelli, V. Cannillo, L. Lusvarghi, M. Montorsi, F. P. Mantini, and M. Barletta, "Microstructural and tribological comparison of HVOF-sprayed and post-treated M-Mo-Cr-Si (M = Co, Ni) alloy coatings," *Wear*, vol. 263, no. 7–12, pp. 1397–1416, 2007.

[19] S. H. Zhang, T. Y. Cho, J. H. Yoon et al., "Characterization of microstructure and surface properties of hybrid coatings of WC-CoCr prepared by laser heat treatment and high velocity oxygen fuel spraying," *Materials Characterization*, vol. 59, no. 10, pp. 1412–1418, 2008.

[20] T. S. Sidhu, S. Prakash, and R. D. Agrawal, "Hot corrosion resistance of high-velocity oxyfuel sprayed coatings on a nickel-base superalloy in molten salt environment," *Journal of Thermal Spray Technology*, vol. 15, no. 3, pp. 387–399, 2006.

[21] T. S. Sidhu, S. Prakash, and R. D. Agrawal, "Study of molten salt corrosion of high velocity oxy-fuel sprayed cermet and nickel-based coatings at 900°C," *Metallurgical and Materials Transactions A*, vol. 38, no. 1, pp. 77–85, 2007.

[22] T. S. Sidhu, A. Malik, S. Prakash, and R. D. Agrawal, "Oxidation and hot corrosion resistance of HVOF WC-NiCrFeSiB coating on Ni- and Fe-based superalloys at 800°C," *Journal of Thermal Spray Technology*, vol. 16, no. 5-6, pp. 844–849, 2007.

[23] B. Lotfi, "Elevated temperature oxidation behavior of HVOF sprayed TiB_2 cermet coating," *Transactions of Nonferrous Metals Society of China*, vol. 20, no. 2, pp. 243–247, 2010.

[24] F. H. Yuan, Z. X. Chen, Z. W. Huang, Z. G. Wang, and S. J. Zhu, "Oxidation behavior of thermal barrier coatings with HVOF and detonation-sprayed NiCrAlY bondcoats," *Corrosion Science*, vol. 50, no. 6, pp. 1608–1617, 2008.

[25] P. Fauchais, M. Fukumoto, A. Vardelle, and M. Vardelle, "Knowledge concerning splat formation: an invited review," *Journal of Thermal Spray Technology*, vol. 13, no. 3, pp. 337–360, 2004.

[26] T. S. Sidhu, S. Prakash, and R. D. Agrawal, "Studies on the properties of high-velocity oxy-fuel thermal spray coatings for higher temperature applications," *Materials Science*, vol. 41, no. 6, pp. 805–823, 2005.

[27] T. S. Sidhu, S. Prakash, and R. D. Agrawal, "Characterizations and hot corrosion resistance of Cr_3C_2-NiCr coating on Ni-base superalloys in an aggressive environment," *Journal of Thermal Spray Technology*, vol. 15, no. 4, pp. 811–816, 2006.

[28] R. A. Neiser, M. F. Smith, and R. C. Dykhuizen, "Oxidation in Wire HVOF-Sprayed Steel," *Journal of Thermal Spray Technology*, vol. 7, no. 4, pp. 537–545, 1998.

[29] S. N. Tiwari and S. Prakash, "Studies on the hot corrosion behavior of some superalloys," in *Proceedings of the Symposium on Localised Corrosion and Environmental Cracking (SOLCEC '97)*, Kalpakkam, India, January 1997.

[30] H. Singh, D. Puri, and S. Prakash, "An overview of Na_2SO_4 and/or V_2O_5 induced hot corrosion of Fe- and Ni-Based superalloys," *Reviews on Advanced Materials Science*, vol. 16, no. 1-2, pp. 27–50, 2007.

[31] D. C. Bolles, "HVOF thermal spraying: an alternative to hard chrome plating," *Welding Journal*, vol. 74, no. 10, pp. 31–34, 1995.

[32] S. Kamal, R. Jayaganthan, and S. Prakash, "High temperature cyclic oxidation and hot corrosion behaviours of superalloys at 900°C," *Bulletin of Materials Science*, vol. 33, no. 3, pp. 299–306, 2010.

[33] D. Toma, W. Brandl, and U. Köster, "The characteristics of alumina scales formed on HVOF-sprayed MCrAlY coatings," *Oxidation of Metals*, vol. 53, no. 1-2, pp. 125–137, 2000.

[34] G. Sreedhar, M. M. Alam, and V. S. Raja, "Hot corrosion behaviour of plasma sprayed YSZ/Al_2O_3 dispersed NiCrAlY coatings on Inconel-718 superalloy," *Surface and Coatings Technology*, vol. 204, no. 3, pp. 291–299, 2009.

[35] S. M. Jiang, X. Peng, Z. B. Bao et al., "Preparation and hot corrosion behaviour of a MCrAlY + AlSiY composite coating," *Corrosion Science*, vol. 50, no. 11, pp. 3213–3220, 2008.

[36] Z. B. Bao, Q. M. Wang, W. Z. Li et al., "Preparation and hot corrosion behaviour of an Al-gradient NiCoCrAlYSiB coating on a Ni-base superalloy," *Corrosion Science*, vol. 51, no. 4, pp. 860–867, 2009.

[37] R. A. Mahesh, R. Jayaganthan, and S. Prakash, "Evaluation of hot corrosion behaviour of HVOF sprayed NiCrAl coating on superalloys at 900°C," *Materials Chemistry and Physics*, vol. 111, no. 2-3, pp. 524–533, 2008.